Lysyl Oxidase-like 2 (LOXL2) and E47 EMT factor: Novel partners in E-cadherin repression and early metastasis colonization

Giacomo Canesin[a,*,#], Eva P. Cuevas[a,#], Vanesa Santos[a], Celia López-Menéndez[a], Gema Moreno-Bueno[a,b], Yujie Huang[c], Katalin Csiszar[d], Francisco Portillo[a], Héctor Peinado[c], David Lyden[c] and Amparo Cano[a,□]

a. Departamento de Bioquímica, Universidad Autónoma de Madrid (UAM), Instituto de Investigaciones Biomédicas "Alberto Sols" CSIC-UAM, IdiPAZ, Madrid, Spain.

b. Fundación MD Anderson International Madrid. 28033 Madrid, Spain

c. Department of Pediatrics, Cell and Developmental Biology, Weill Cornell Medical College, New York, NY 10021, USA.

d. John A Burns School of Medicine, University of Hawaii, Honolulu, HI 96822, USA.

*. Present address:

Divisions of Cell and Experimental Pathology and Urology, Lund University, Clinical Research Centre, Skåne University Hospital, SE-20502 Malmö (Sweden).

# Equal contribution

□ Corresponding author:

Amparo Cano. Departamento de Bioquímica, Universidad Autónoma de Madrid (UAM)

Instituto de Investigaciones Biomédicas "Alberto Sols" CSIC-UAM, Arzobispo Morcillo, 2, 28029 Madrid, Spain. Tel: +34-91-4975400. Fax: +34-91-5854401. acano@iib.uam.es

Short title: E47 and LOXL2 contribute to early metastasis

Word length: 5,258 words

ABSTRACT

Epithelial–mesenchymal transition (EMT) has been associated with increased aggressiveness and acquisition of migratory properties providing tumor cells with the ability to invade into adjacent tissues. Downregulation of *E-cadherin*, a hallmark of EMT, is mediated by several transcription factors (EMT-TFs) that act also as EMT inducers; among them, Snail1 and the bHLH transcription factor E47. We previously described lysyl oxidase-like 2 (LOXL2), a member of the lysyl oxidase family, as a Snail1 regulator and EMT inducer. Here we show that LOXL2 is also an E47 interacting partner and functionally collaborates in the repression of *E-cadherin* promoter. Loss and gain of function analyses combined with *in vivo* studies in syngeneic breast cancer models demonstrates the participation of LOXL2 and E47 in tumor growth and their requirement for lung metastasis. Furthermore, LOXL2 and E47 contribute to early steps of metastatic colonization by cell and non-cell autonomous functions regulating the recruitment of bone marrow progenitor cells to the lungs and by direct transcriptional regulation of fibronectin and cytokines TNFα, ANG-1, and GM-CSF. Moreover, fibronectin and GM-CSF proved to be necessary for LOXL2/E47 mediated modulation of tumor growth and lung metastasis.

Keywords: E47, LOXL2, E-cadherin, EMT, pre-metastastic niche, metastasis colonization, fibronectin, GM-CSF

Introduction

Epithelial–Mesenchymal transition (EMT), an essential process in development, has been established as a key event for early metastatic stages. It provides tumor cells with the ability to invade into adjacent tissues and to promote their intravasation and extravasation (1-3). Downregulation of *E-cadherin* is a hallmark of EMT, leading to the loss of cell-cell interactions and apical–basal cell polarity required for the acquisition of a motile and invasive cell behavior (1, 4). Several transcription factors have been described as EMT inducers, including members of the Snail, bHLH and ZEB families (EMT-TFs) (5, 6). Among the bHLH factors, E47 (encoded by the *E2A* gene) is an EMT-TF (7-9).

EMT-TFs are regulated at both transcriptional and post-transcriptional levels, including miRNAs and post-translational regulatory mechanisms that impinge on the stability, nuclear localization and/or functional activity (6, 10). Lysyl oxidase-like 2 (LOXL2) regulates Snail1 stability, and contributes to EMT induction by Snail1-dependent and -independent mechanisms (11-13). LOXL2 is a member of the lysyl oxidase (LOX) family, constituted by the prototypical LOX and four related members (LOXL1-4) (14) sharing a conserved catalytic domain required for the oxidative deamination of peptidyl-lysine residues in substrates generating covalent inter- and intramolecular crosslinks during extracellular matrix assembly (14-16). Most of the LOX family members have also been implicated in tumorigenesis (17). LOXL2 has been shown to be involved in invasion of breast carcinoma and associated to poor clinical outcome and metastasis in (N0) and ER(-) breast tumors (13, 18, 19). Intracellular accumulation of LOXL2 is a prognostic marker in head and neck squamous cell carcinomas (12) and is associated to distant metastasis of basal breast carcinoma (13). However, little is known about LOXL2 functions in early metastatic events.

Pre-metastatic niche formation is an essential event for early tumor cell homing and eventual colonization of secondary organs (20). It involves a complex network of tumor-host interactions,

secretion of soluble factors and exosomes that mediate the remodeling of the extracellular matrix and the recruitment of bone marrow derived cells (BMDC) into target organs (20-22). Secreted LOX and hypoxia are relevant to metastasis and pre-metastatic niche formation in breast cancer (23, 24) and hypoxia-induced LOXL2 and LOXL4 also contribute to the recruitment of BMDC by specific breast carcinoma cells (25).

Results we describe here demonstrate that LOXL2 interacts with E47 to collaborate in down-regulation of *E-cadherin* transcription. We also show that interference with either factors decreases the metastatic potential of highly malignant breast cancer cells concomitant with a marked reduction in the mobilization and recruitment of bone marrow progenitor cells (BMPC) to pre-metastatic sites. Furthermore, LOXL2 and E47 downregulation impairs transcriptional expression of fibronectin and multiple cytokines at primary tumors and/or metastatic lungs. Noticeably, LOXL2 or E47 actions in these processes depend on fibronectin and GM-GSF but are independent of other LOX members, thus demonstrating novel and specific functions for LOXL2 and E47 proteins in breast cancer metastasis.

RESULTS

E47 and LOXL2 interact and collaborate in *E-cadherin* promoter repression

In order to identify partner(s) interacting with E47, we performed a two-hybrid screen resulting in the identification of LOXL2 (data not shown). Co-immunoprecipitation assays in stable MDCK-EGFP-E47 cells (9) transiently transfected with LOXL2-Flag indicated that LOXL2 and E47 interact *in vivo* (Figure 1a). *In vitro* pull-down assays confirmed interaction between GST-E47 and LOXL2-Flag (Figure 1b). Immunofluorescence analysis showed that LOXL2 co-localizes with E47 in the perinuclear region (Figure 1c), as reported for LOXL2 and Snail1 (11). Importantly, interaction of endogenous LOXL2 and E47 proteins was confirmed by co-immunoprecipitation in two breast carcinoma cell lines, mouse Eo771 and human MDA-MB231 cells (Figure 1d).

As we have recently observed that E47 induced a dose dependent repression of *E-cadherin* promoter activity (9), we tested the functional consequence of LOXL2/E47 interaction on the regulation of the *E-cadherin* promoter. Interestingly, E47-mediated repression was increased by 50% in the presence of LOXL2 (Figure 1e), indicating that E47 and LOXL2 collaborate in *E-cadherin* repression, similar to Snail1 and LOXL2 (11), in full agreement with the binding of both factors to the endogenous *E-cadherin* promoter (9, 26). Accordingly, E-cadherin is not detected in cells expressing LOXL2 and E47 (Figure 1c). Deletion of the AD1 transactivation domain of E47 (E47ΔAD1 mutant), required for recruitment of co-factors (27), abolished *E-cadherin* promoter repression, but co-transfection of LOXL2 with E47ΔAD1 restored promoter repression (Figure 1e). The collaboration between LOXL2 and E47 proved to be also independent of LOXL2 catalytic activity (Figure 1f).

These data indicate that E47 and LOXL2 interact and collaborate in the repression of the *E-cadherin* promoter independently of the E47 AD1 domain and LOXL2 catalytic activity.

E47 or LOXL2 silencing influences the expression of EMT markers and some of the LOX members

The implication of some EMT-TFs as well as LOXL2 in breast cancer models (3, 5, 18) and association of E2A expression in N0 breast carcinomas (9) has been previously shown. To explore the significance of E47 and LOXL2 in breast cancer, we analyzed their expression in two syngeneic mouse breast carcinoma models, Eo771 and 4T1 cells. Mesenchymal Eo771 cells, derived from C57BL/6J breast carcinoma (28), express both E47 and LOXL2, while epithelial 4T1 cells, derived from Balb/C breast carcinoma, only express E47 and maintain E-cadherin expression (Supplementary Figure S1).

To examine the role of E47 and LOXL2, we first generated Eo771 cells stably expressing mCherry and Luciferase (Eo771mCherryLuc) in which LOXL2 or E47 were stably silenced. We selected two short hairpin RNA sequences against E47 (shE47) and LOXL2 (shLOXL2) and stable derived pools and clones for further analysis showing 60-80% decrease in E47 or LOXL2 expression (Supplementary Figure S2). While LOXL2 silencing did not influence E47 expression, E47 silencing induced a decrease of LOXL2 protein (Supplementary Figure S2a and b), suggesting the involvement of post-transcriptional regulation.

Analysis of EMT markers showed that E47 knockdown in Eo771 cells decreased Snail2 and ZEB1 expression but LOXL2 silencing did not affect the expression of those EMT-TFs (Supplementary Figure S2b). No expression of Snail1 was observed in Eo771 cells. Both shE47 and shLOXL2 cells exhibited a strong decrease in fibronectin expression, but no change in E-cadherin expression (Supplementary Figure S2a and b) and maintained a mesenchymal-like phenotype (not shown).

We further tested for any expression change of LOX members. Eo771-shE47 cells displayed *LOX* upregulation, and shLOXL2 cells showed *LOX* and *LOXL3* upregulation, but no significant differences in *LOXL1* or *LOXL4* transcripts (Supplementary Figure S3a). Upregulation of LOXL3 protein levels resulting from either LOXL2 or E47 silencing was confirmed both in cell extracts and conditioned media, and a slight increase was observed in secreted LOX protein after E47 silencing

(Supplementary Figure S3b and c). Interestingly, LOXL2 was not detected in the conditioned media from parental Eo771 cells nor any of the derived clones (Supplementary Figure S3c), suggesting that Eo771 cells do not secrete LOXL2 as confirmed in conditioned media from transiently transfected Eo771 cells in which LOXL2-HA was barely detected (Supplemental Figure S3d). These data show that LOXL2 or E47 silencing in Eo771 cells induces the expression of LOXL3 and/or LOX and the decrease of EMT markers fibronectin, Snail2 or ZEB1, without apparent effect on the phenotype.

E47 or LOXL2 silencing reduces tumor growth and decreases lung metastasis.

To investigate the role of E47 and LOXL2 in the tumorigenic and metastatic behavior of Eo771 cells, spontaneous metastasis assays were performed in syngeneic mice. Eo771 parental, shE47, shLOXL2 and control cells were injected into the mammary fat pad (mfp) of C57BL/6J mice. Tumors started to develop 7 days post-injection (dpi) in all groups but those derived from shE47 and shLOXL2 cells grew more slowly than controls (Figure 2a and b; Supplementary Figure S4a and b). Since no differences in tumor growth or histology were found between the two control groups, pGIPZ and pLKO (data not shown), we refer most of the following analyses to pLKO control. Histological analysis of tumors showed that parental and pLKO cells induce undifferentiated tumors with loose intercellular contacts and little stromal component, and silencing of LOXL2 or E47 did not significantly change tumor histology (Figure 2c, left panels). Analysis of mice at necropsy 24 dpi showed spontaneous lung metastasis reduced to 90% in Eo771-shLOXL2 and 55% in -shE47 injected mice (Figure 2d and e; Supplementary Figure S4c). Histological lung analyses demonstrated that macrometastases where only detected in control cells (Figure 2c, right panels, and data not shown). Similar results were obtained in experimental metastasis assays (tail vein injection) where lung metastatic lesions were reduced 95% and 75% in Eo771shLOXL2- and shE47-injected mice, respectively (Figure 2f and g). Together, these data indicate that E47 and LOXL2 are

required for lung metastasis of Eo771 cells independently of their tumor growth suppressive effects. To further analyze the LOXL2/E47 collaboration, and because of the inability to obtain double knockdown cells due to cell viability, a rescue experiment was performed overexpressing LOXL2 in Eo771-shE47 cells (Supplementary Figure S2d). LOXL2 expression did not significantly change tumor growth, histology, or metastatic burden (Figure 2h-j), suggesting that both factors are jointly required for Eo771 tumorigenenic and metastatic potential. To confirm the collaboration of LOXL2 and E47 in and independent model, similar studies were performed in 4T1 cells. Because these cells only express E47 (Supplementary Figure S1) a double approach was followed: knockdown of E47 and overexpression of LOXL2. E47 silencing in 4T1 cells did not change E-cadherin or Snail1/2 expression while LOXL2 expression modestly decreased E-cadherin expression (Figure 3a and g). Injection of manipulated 4T1 cells in syngeneic Balb/C mice indicated that E47 depletion strongly decreased tumor growth and lung metastasis (Figure 3 b-f) while overexpression of LOXL2 did not significantly affect tumor growth or metastatic burden as determined by bioluminescence (Figure 3h-j), but increased the size of lung metastasis compared to controls (Figure 3f). No changes in tumor histology were observed after manipulation of either E47 or LOXL2 in 4T1 cells (Figure 3f, lower panels). These data support the collaboration of LOXL2 and E47 in promoting an aggressive phenotype in breast cancer cells.

LOXL2 and E47 are required for early metastatic colonization

To explore the mechanisms involved in metastatic suppression by E47 and LOXL2 silencing, we studied the implication of these proteins in metastatic niche formation and early stages of metastasis. Towards this aim, we first analyzed the recruitment of BMDC to metastatic organs in the Eo771 model using GFP bone marrow transplanted C57BL/6J mice (21). Parental Eo771, pLKO, shE47 and shLOXL2 cells were injected into the mfp and mice where sacrificed 15 dpi when Eo771 tumor cells were first detected in lungs (Supplementary Figure S5). Lungs were analyzed for

BMDC-GFP$^+$ infiltration and the presence of metastatic Eo771-mCherry$^+$ cells. About 10% of GFP$^+$ cells were recruited to the lungs of non-injected mice (Figure 4b). Lungs of mice carrying parental Eo771 or Eo771-pLKO tumors showed a 7-10 fold increase in the infiltrated BMDC-GFP$^+$ and contained clusters of metastatic mCherry$^+$ cells co-localizing with GFP$^+$ cells (Figure 4a, panels a-f, 4b and c). In lungs from mice bearing shLOXL2 or shE47 tumors BMDC-GFP$^+$ infiltration regressed to basal levels (Figure 4a, panels g-l, 4b and c). We then analyzed the BMDC populations mobilized to the blood and recruited to the lungs and the primary tumors of C57BL/6J mice injected with Eo771 interfered cells at 15 dpi. We focused on bone marrow progenitor (BMPC, c-kit$^+$/Sca-1$^+$) and myeloid cell populations (CD11b$^+$/Gr1$^+$) because of their reported involvement in pre-metastatic niche formation (21, 29). We first tested whether the inhibitory effects of GFP on the immune response of 4T1 cells in Balb/C mice (30) could affect Eo771 cells, since shLOXL2 was cloned into pGIPZ-GFP vector. Both myeloid and BMPC populations increased in blood and lungs of C57BL/6J mice injected with Eo771-pLKO and -pGIPZ cells compared to non-injected cells, with no significant differences between the two groups (Supplementary Figure S6); thus we used pLKO cells as controls in subsequent analyses. Silencing of LOXL2 or E47 in Eo771 cells affect neither myeloid cell mobilization nor their lung recruitment (Figure 5a and b). In contrast, BMPC mobilized to the blood were reduced in mice bearing Eo771-shLOXL2 or shE47 tumors (Figure 5d). Moreover, BMPC levels in the lungs of Eo771-shLOXL2 or shE47 mice were similar to non-injected mice (Figure 5e). Noticeably, LOXL2 expression in Eo771-shE47 cells increased BMPC lung recruitment to levels similar to pLKO control cells without altering myeloid cell recruitment (Figure 5c and f). Similar findings were obtained in 4T1-LOXL2 cells where the BMPC population increased in blood and lungs of Balb/C-injected mice without modification in the myeloid population (Figure 5i, j, m and n); an apparent reverse situation was found in 4T1-shE47-bearing mice showing a significant decrease of myeloid cells and increased BMPC in lungs without changes in blood mobilization of either population (Figure 5g, h, k and l). No significant differences in

myeloid cells or BMPCs recruitment to primary tumors were detected among the different groups and controls (Supplementary Figures S6 and S7).

These data indicate that LOXL2 and/or E47 are required for the mobilization and lung recruitment of different populations of bone marrow-derived cells dependent on the specific metastatic microenvironment.

LOXL2 and E47 modulate the expression of fibronectin and cytokines during formation of the metastatic niche

Fibronectin, LOX and various cytokines have been previously implicated in pre-metastatic niche formation (20-22, 29, 31). We therefore studied the influence of LOXL2 and E47 on the expression of these factors during early metastatic stages. We first performed qPCR analysis in the primary tumors and lungs of mice injected with Eo771-pLKO, shLOXL2 and shE47 cells at 15 and 24 dpi (early colonization and end-point of the experiment, respectively; Supplementary Figure S5). Silencing of E47 and LOXL2 in primary tumors at both time points was confirmed (Figure 6a; Supplementary Figure S8a and b). Both *LOXL2* and *E47* levels were decreased in Eo771-shE47 and shLOXL2 tumors, suggesting a crosstalk between these two factors within the tumor context. In the lungs, no significant differences in *LOXL2* expression were observed in different groups at 15 dpi (Figure 6b), indicating the probable contribution of stromal LOXL2. However, very low levels of *LOXL2* were detected in the lungs of mice bearing Eo771-shLOXL2 or shE47 tumors 24 dpi (Supplementary Figure S8c). Upregulation of *LOX* and/or *LOXL3* was also detected in primary tumors and lungs of Eo771-shE47 or shLOXL2 mice at 15 and 24 dpi without changes in *LOXL1* or *LOXL4* expression (Figure 6a and b; Supplementary Figure S8b and c), as observed in cell cultures (Figure S3a).

Fibronectin expression was strongly decreased in tumors and lungs of Eo771-shLOXL2 or shE47 mice (Figure 6a and b; Supplementary Figure S8a and c) as compared to controls. Overexpression

of LOXL2 in Eo771-shE47 cells did not significantly modify the expression of *fibronectin* or of other *LOX* member (Figure 6c and data not shown). However, in the lungs of Balb/C mice bearing 4T1-LOXL2 cells, increased *fibronectin* expression as well as *E47*, *LOXL1*, and *LOXL3* was detected mainly (Figure 6d). In contrast, although decreased *LOXL1* and L*OXL2* was found in tumors of 4T1-shE47 mice, increased expression of all *LOX* members was detected in lungs (Supplementary Figure S9), suggesting a more complex regulation in the absence of both E47 and LOXL2.

To identify the cytokines involved, we first tested the conditioned media from Eo771-interfered cells in a cytokine array. Granulocyte-Monocyte Colony Stimulating Factor (GM-CSF) and Angiopoietin-1 (ANG-1) were decreased in the conditioned media from both Eo771-shLOXL2 and shE47 cells (Figure 7a). The down-regulation of GM-CSF and ANG-1 was confirmed by qPCR in cultured cells, primary tumors, and lungs from Eo771-shE47/shLOXL2-injected mice at 15 and 24 dpi (Figure 7b-d; Supplementary Figure S8d and e). We also analyzed the expression of cytokines previously related to the recruitment of BMDC and pre-metastatic niche formation, Transforming Growth Factor β (TGFβ), Tumor Necrosis Factor α (TNFα), S100A8/S100A9 and tenascin-C (TEN-C) (29, 31, 32). E47 or LOXL2 silencing induced a marked decrease in *TNFα* expression in Eo771 cells, tumors and lungs (15 and 24 dpi) while no differences were detected for TGFβ and TEN-C expression (Figure 7b-d; Supplementary Figure S8d and e). Additionally, S100A8/S100A9 expression was strongly downregulated in lungs from Eo771-shLOXL2 or shE47-injected mice (Figure 7d; Supplementary Figure S8f). Lung expression of TNFα, GM-CSF and ANG-1 was restored to varying levels after LOXL2 overexpression in Eo771shE47 cells (Figure 7e). Similar analyses in Balb/C mice injected with 4T1 cells manipulated for LOXL2 or E47 expression indicated the contribution of LOXL2 and E47 to cytokine expression; strong upregulation of GM-CSF and downregulation of S100A8/S100A9 levels were detected in lungs from 4T1-LOXL2 (Figure 7f) and 4T1-shE47-injected mice, respectively, although upregulation of GM-CSF was also observed in 4T1-shE47 cells (Supplementary Figure S9c).

The LOXL2 and E47 regulation of some cytokines was further explored at promoter level in the Eo771 system. The activity of *TNFα* and *GM-CSF* promoters was strongly decreased in Eo771-shLOXL2 and shE47 cells in the absence and presence of PMA (a TNFα inducer) (Figure 7g and i) supporting transcriptional regulation. Indeed, transient assays in Eo771 cells indicated that E47 upregulated the *TNFα* promoter in a dose-dependent fashion; although LOXL2 alone had no effect, together with E47 it induced a synergistic activation of the *TNFα* promoter (Figure 7h). Analyses of the *GM-CSF* promoter showed that LOXL2 induced a significant upregulation while E47 did not modify promoter activity in the absence or presence of LOXL2 (Figure 7j).

Together, these data demonstrate that LOXL2 and E47 transcriptionally regulate the expression of fibronectin, GM-CSF, TNFα, ANG-1 and/or S100A8/S100A9 in primary tumors and metastatic lungs of breast carcinoma models.

LOXL2 and E47 take over pre-metastatic niche conditioning and depend on fibronectin and GM-CSF.

We next analyzed whether the pro-metastatic actions of LOXL2 and E47 depend on a pre-metastatic niche conditioning (21, 29). To this end, shE47 and shLOXL2-Eo771-mCherryLuc cells were tail vein injected in mice-bearing Eo771 tumors at 10 dpi when a pre-metastatic niche has been prepared in this system (Supplementary Figure S5) and lung metastasis analyzed 15 days later. Silencing of E47 or LOXL2 decreased metastasis burden by 65% and 85%, respectively (Figure 8a and b), indicating a predominant cell autonomous action of LOXL2 and E47 in metastatic colonization.

Finally, the functional contribution of fibronectin and some of the cytokines regulated by LOXL2/E47 was also analyzed. Knockdown of fibronectin in Eo771 cells did not affect tumor growth (data not shown) but significantly reduced lung metastasis (>90%) and GM-CSF and TNFα expression in lungs (Figure 8c-f). On the other hand, GM-CSF silencing strongly reduced tumor

growth and lung metastasis, associated to decreased fibronectin but increased TNFα expression (Figure 8g-k). No significant changes in lung recruitment of BMPC or myeloid cells were detected in Eo771-shGM-CSF bearing mice (Figure 8l), suggesting that GM-CSF is dispensable for BMDC recruitment and might contribute to metastasis through fibronectin regulation.

Altogether, the present data highlight the contribution of LOXL2 and E47 to early metastatic colonization by regulating fibronectin and pre-metastatic cytokines expression.

DISCUSSION

There is currently little information on E47 interacting partners that regulate its activity. Using an unbiased screening approach, we identified LOXL2 as an E47 partner. Our data demonstrate the E47/LOXL2 interaction and identify a new functional cooperation between both factors in the regulation of *E-cadherin* repression. We have partly uncovered the mechanism involved in LOXL2 and E47 co-repression as independent of E47-AD1 domain and LOXL2 catalytic activity that suggest non-conventional mechanisms we are presently investigating. The recently reported binding of both factors to the endogenous *E-cadherin* promoter (9, 26) support their functional co-operation here described. Together with the previously identified Snail1-LOXL2 interaction (11), the present findings indicate that LOXL2 is an important regulator of several EMT-TFs, further corroborating the intracellular role of LOXL2 (11-13).

Our data suggest that E47 and LOXL2 can play differential roles regarding *E-cadherin* repression and EMT induction in distinct cellular context. Thus, LOXL2 or E47 silencing in Eo771 cells decreases fibronectin and Snail2/ZEB1 without inducing E-cadherin expression while overexpression of LOXL2 in 4T1 cells moderately decreases E-cadherin expression. Nevertheless these changes are insufficient to modify the Eo771-mesenchymal or 4T1-epithelial phenotypes, in contrast to other systems, including basal carcinoma cells (9, 11-13), and might be determined by the complementary action of other EMT-TFs in different cellular contexts.

Interestingly, we observed an apparent cross-regulation between E47 and LOXL2 that seems to be influenced by the tumor context, where E47 and LOXL2 could act synergistically in tumor growth and metastasis dissemination as demonstrated in two breast cancer models. Indeed, silencing of LOXL2 or E47 in Eo771 cells induces a mutual downregulation of both factors in tumors, and LOXL2 overexpression in 4T1 cells induces *E47* in metastatic lungs. In fact, initial *E2A* and *LOXL2* promoter analyses support transcriptional cross-regulation by LOXL2 and E47 that deserve further studies (EP Cuevas, unpublished data). LOXL2 participation in lung metastasis dissemination in gastric (33) and breast carcinomas (13, 17, 34) has been associated to extracellular LOXL2. Our results support a new scenario where LOXL2 executes its functions intracellularly since Eo771 cells do not secrete LOXL2 (Supplementary Figure S3), in agreement with our previous studies (11-13). The coordinated action of LOXL2 and E47 in the development of experimental lung metastasis suggests cell-autonomous actions for both factors in lung homing/colonization even in the absence of primary tumors. In fact, LOXL2 and E47 action on metastasis seems to prevail over pre-metastatic niche conditioning supporting a cell-autonomous action of both molecules in early metastasis colonization. Recent data have revealed the requirement of mesenchymal-epithelial transition (MET) for metastasis outgrowth (35-37). Our data suggest that EMT-like processes mediated by LOXL2 and E47 could be a requirement for early metastastic stages before overt macrometastasis appear. This proposal is nevertheless compatible with additional actions of both factors on the metastatic microenvironment. Indeed, the present data show that E47 and/or LOXL2 are needed for the recruitment of BMPC at early metastatic sites. Interestingly, in both Eo771 and 4T1 breast models, BMPC ($ckit^+/Sca1^+$) is the main recruited population compared to myeloid $CD11b^+/Gr\text{-}1^+$ population in response to LOXL2 expression. In fact, myeloid cells were mobilized to the blood and recruited to the lungs in mice bearing Eo771-shLOXL2 and -shE47 tumors as well as in 4T1-LOXL2 tumors. Nevertheless, myeloid cell recruitment decreased after E47 deletion in 4T1 cells, suggesting that, in the absence of LOXL2, E47 might primarily impact on

myeloid population on a Balb/C background. Our data thus suggest that LOXL2 and/or E47 are implicated in the recruitment of the more undifferentiated BMPC population, in agreement with previous reports (21), or myeloid populations (38, 39) depending of the specific metastasis microenvironment. Interestingly, LOXL2 and E47 regulate fibronectin expression in Eo771 cells, as well as in tumors and early metastatic lungs. This finding is relevant, as BMPC are preferentially recruited to lung areas rich in fibronectin (21), furthermore, a fibronectin-enriched extracellular matrix provides a favorable environment for LOX catalytic activity in the pre-metastatic niche (24, 40, 41). Indeed, fibronectin regulation by LOXL2 and E47 seems to be determinant for breast cancer metastatic fitness as indicated by fibronectin knockdown in Eo771 cells. Interestingly, silencing of LOXL2 or E47 induces the upregulation of *LO*X and *LOXL3* at Eo771 primary tumors and early metastatic sites (Figure 6) that could partly explain the myeloid cells recruitment as reported in other breast models (24). Importantly, LOX upregulation and myeloid cell recruitment do not compensate for the absence of LOXL2 or E47 for development of micrometastases, indicating a dominant role for these proteins at early metastatic stages. Preliminary analyses of Eo771-tumor extracellular matrix suggest no major changes in collagen deposition or organization in response to E47 and LOXL2 silencing or overexpression (data not shown). We therefore postulate that an E47/LOXL2-dependent mechanism is involved in fibronectin deposition and BMPC recruitment to early metastatic sites, while LOX-dependent mechanisms would execute myeloid cell recruitment and cross-linking of extracellular matrix in specific metastasis microenvironments. The present results indicate that LOXL2 and E47 also regulate the expression of GM-CSF, TNFα and ANG-1, in primary tumor and lungs, factors that contribute to BMDC recruitment and pre-metastatic niche (20, 21). The transcriptional downregulation of *TNFα* and *GM-CSF* promoters by LOXL2 and E47 in Eo771 cells, together with inhibition of metastasis colonization following GM-CSF knockdown might well explain the remarkable effect of both factors in early metastatic colonization, further reinforcing the intracellular action of LOXL2.

Interestingly, GM-CSF knockdown strongly suppressed fibronectin expression in lungs without affecting BMPC recruitment. In contrast, a marked decrease in GM-CSF and TNFα expression occurs after fibronectin silencing, suggesting a coordinated action of LOXL2/E47 in the regulation of fibronectin through GM-CSF. Interestingly, LOXL2 or E47 silencing also dramatically reduced S100A8/S100A9 expression in lungs, indicating that at least in Eo771 and 4T1 models these cytokines could be involved in the recruitment of BMDC at early metastatic sites.

The present results extend recent data from Wong et al. reporting that under hypoxia, secreted LOXL2 in human breast cancer cells induce BMDC lung infiltration and colonization of metastatic cells by influencing the extracellular matrix (25). Moreover, our results support novel cell-autonomous actions of LOXL2 and suggest that high levels of LOXL2 as those present in Eo771 cells or in human basal-like carcinoma cells (13) can be sufficient to promote early metastasis colonization. Noticeably, high LOXL2 levels in breast carcinoma cells associate to a mesenchymal phenotype (13, present data), further suggesting that EMT mediated by LOXL2 favors initial lung homing and can over-impose on pre-metastatic niche formation. This scenario, together with the upregulation of E47 observed in primary N0 breast carcinomas (9) provides additional mechanisms for metastasis progression in breast tumors.

MATERIALS AND METHODS

Cell culture

Human HEK293T and MDA-MB-231, dog MDCK, and mouse Eo771 and 4T1 cell lines were obtained from the American Type Culture Collection. MDCK-EGFP-E47 and MDCK-LOXL2-Flag cells were previously described (9, 11). Eo771-mCherryLuc and 4T1-mCherryLuc cells were obtained by

lentiviral infection with PRRL-cPTT-PGK-mCherry-W vector. All cell lines were grown according to American Type Culture Collection specifications.

Vectors

Mouse pcDNA3-E47, human pReceiver-LOXL2-HA and mouse pcDNA3-LOXL2-Flag and LOXL2-ΔCat-Flag vectors have been previously described (9, 13, 26). pZeo-E47 vector was obtained by subcloning mouse E47 cDNA into the pZeo vector, from which the pZeo-ΔAD1-E47 vector was generated by deletion of nt 1 to 279 (a.a. 1-93).

Two-hybrid screen.

The two-hybrid screen was performed as described (7) using the bHLH domain of E47 as bait. One of the isolated prays corresponded to the cDNA sequence of LOXL2 catalytic domain.

RNA interference.

Selected shRNAs sequences were: TRCN00002-33414 and TRCN0000233416 for mouse E47; and TRCN0000054618 and TRCN0000054619 for mouse GM-CSF (Sigma-Aldrich); sc-35371-V for mouse fibronectin (Santa Cruz Biotechnology, Inc.); and V3LMM_455747 for mouse LOXL2 (Open Biosystem. Controls pLKO and pGIPZ were from Sigma-Aldrich and Open Biosystem, respectively. Stable transfectants were selected with 3 μg/mL puromycin for 2-3 weeks. At least two independent pools and/or clones were isolated from each transfection and used for further analysis.

Transient transfections.

Transfections were performed with Lipofectamine 2000 (Life Technologies) following manufacturer's instructions.

Co-immunoprecipations, pull down assays and Western-Blot.

Cell extracts were obtained using IPH buffer (50 mM Tris-HCl pH 8.0, 150 mM NaCl, 5 mM EDTA, 0.5% NP-40) supplemented with proteases and phosphatases inhibitors (2mM PMSF, 2 μg/ml leupeptin, 20 ng/ml aprotinin, 1 mM sodium orthovanadate). Co-immunoprecipitations and pull-downs assays were performed as described (9, 11) and blots were incubated with the indicated primary and secondary-HRP-conjugated antibodies (listed in Supplementary Table S1)**.**

Promoter analysis.

Mouse *E-cadherin* promoter assays were performed as described (26, 42). For *TNFα* and *GM-CSF* promoters, Eo771 cells and derived sh-clones were transiently transfected with mouse TNFα-luciferase construct (pGL3-mTNF) (provided by Dr. M. Fresno, CBMSO, Madrid, Spain) or mouse GM-CSF-luciferase construct (pMGM0.2-luc) (provided by Dr. PN. Cockerill, St. James's University Hospital, Leeds, UK) and the indicated amounts of pcDNA3-LOXL2-Flag and/or pcDNA3-E47 vectors, and co-transfected with 10 ng of CMV-βgal. When indicated, cells were treated with 100 nM PMA 18h prior to lysis.

Cytokine array.

Secreted factors in conditioned media were detected using the mouse angiogenesis antibody proteome profiler array (#ARY015, R&D Systems), following manufacturer's instructions.

Semiquantitative and quantitative PCR studies.

Total RNA from cell lines was extracted with Trizol (Life technologies) as described (42). Disruption of frozen tumors and lungs was performed also in Trizol using a politron device. Two micrograms

of RNA were treated with DNaseI and used for cDNA synthesis (42). Semiquantitative-PCR or quantitative-PCR were performed using pre-designed TaqMan© probes or SybrGreen PCR reagents (Sigma-Aldrich) on an iQ5 iCycler Realtime PCR Detection System (BioRad). Primers and probes sequences,and amplification conditions are indicated in Supplementary Tables S2 and S3. Relative expression was normalized to β-actin or GAPDH.

Flow cytometry.

Lung and primary tumor tissues were prepared as previously described (43). Peripheral blood was obtained by retro-orbital bleeding directly into anti-coagulant tubes. Cell suspensions were incubated with the following fluorescent primary antibodies (Supplementary Tables S1) for 45 min and fixed in 2% PFA over-night. Fluorescence was measured using a FACSCalibur cytometer with CellQuest software (BD). FACS data were analyzed with FlowJo software (TreeStar).

Immunofluorescence confocal microscopy.

Immunofluorescence of cells fixed in 4% paraformaldehyde was performed as described (42). For tissue fluorescence, mice tissues were fixed overnight in 2% PFA:20% sucrose mix and cryoembedded in Tissue-tek OCT. Sections (5 µm) were stained with DAPI. GFP and mCherry-positive cells were detected by their intrinsic signal. Fluorescent images were obtained using a Leica TCS-SP5 confocal microscope and analyzed using the Leica LAS-AF program. Digital images of mCherry/GFP stained sections were analyzed and pixels were quantified with ImageJ Software (NIH).

Animal experimentation and *in vivo* imaging.

For tumor induction and spontaneous metastasis assays, parental Eo771- and 4T1-mCherryLuc cells and derived clones were orthotopically injected ($1x10^6$ in 0.1 ml serum free growth medium)

into the left fifth mfp of 8 weeks-old C57BL/6J and Balb/C mice, respectively. Tumor growth was measured once a week by determination of the two orthogonal external diameters using a caliper and by bioluminescence. Tumors were surgically excised between 15 and 28 dpi. Bone marrow (BM) transplantation was performed as described (43). For experimental metastasis assays Eo771-mCherryLuc cells and derived clones were injected ($1x10^5$ in 0.1 ml serum free growth medium) into the tail vein of 8 weeks-old C57BL/6J mice. Pre-conditioning experiments were performed as described (29); briefly, wild type Eo771 cells (without any labeling) were implanted into mfp of female 8-weeks C57BL/6J mice and 10 days later, Eo771pLKO-, shLOXL2-, or shE47--luciferase labeled cells were injected by tail. Lungs were removed for bioluminescence at 25 dpi of parental cell injection.

Live animal bioluminescence optical imaging was performed using the IVIS Spectrum system or the IVISR Lumina II system (Caliper, Xenogen) (13). At the end-point of the experiments, mice were euthanized 5 min later of *in vivo* bioluminiscent measure, and organs analyzed for luciferase expression. Data were quantified with the Living Imaging software 4.2 (Xenogen Corporation). Tissues were dissected, fixed in 10% formalin and embedded in parafim for hematoxylin/eosin staining, or snap-frozen in liquid nitrogen for RNA extraction. All mouse work was performed in accordance with institutional, IACCUC, AAALAS and UAM guidelines and approved by the corresponding Use Committee for Animal Care.

Statistical analysis.

Mouse experiments were performed in duplicate, using at 4-6 mice per treatment group. All the *in vitro* experiments were performed at least twice. Statistical analyses were carried out using Graph Pad Prism software and statistical significance was determined by ANOVA or two-tailed Student's t test**.**

Acknowledgments. The authors thank members of A. Cano's group: Saleta Morales and Amalia Montes for technical support, Ana Villarejo and Fernando Salvador for help in flow cytometry and collagen cross-linking analyses, and Thomas Look, Manuel Fresno and Peter N. Cockerill for providing reagents, and Angela Nieto for reading the manuscript. The work was supported by the Spanish Ministry of Science and Innovation (SAF2010-21143; Consolider 2007-CS00017); AICR (12-1057) and ISCIII (RETIC- RD12/0036/0007) to AC, and Comunidad de Madrid (S2010/BMD-2302) to AC and GMB.

Conflict of Interest. The authors declare no conflict of interest

Supplementary Information accompanies the paper on the Oncogene website (http://www.nature.com/onc).

REFERENCES

1. Thiery JP, Acloque H, Huang R, Nieto MA. Epithelial-mesenchymal transitions in development end disease. *Cell* 2009; **139**: 871-890.
2. Polyak K, Weinberg RA. Transitions between epithelial and mesenchymal states: acquisition of malignant and stem cell traits. *Nat Rev Cancer* 2009; **9**: 265-273.
3. Nieto MA. The ins and outs of the epithelial to mesenchymal transition in health and disease. *Annu Rev Cell Dev Biol* 2011; **27**: 347-376.
4. Moreno-Bueno G, Portillo F, Cano A. Transcriptional regulation of cell polarity in EMT and cancer. *Oncogene* 2008; **27**: 6958-6969.

5. Peinado H, Olmeda D, Cano A. Snail, Zeb and bHLH factors in tumor progression: an alliance against the epithelial phenotype? *Nat Rev Cancer* 2007; **7**: 415-428.

6. Nieto MA, Cano A. The epithelial–mesenchymal transition under control: Global programs to regulate epithelial plasticity. *Sem Cancer Biol* 2012; **22**: 361-368.

7. Perez-Moreno MA, Locascio A, Rodrigo I, Dhondt G, Portillo F, Nieto MA *et al*. A new role for E12/E47 in the repression of E-cadherin expression and epithelial mesenchymal transitions. *J Biol Chem* 2001; **276**: 27424-27431.

8. Peinado H, Marin F, Cubillo E, Stark HJ, Fusenig N, Nieto MA *et al*. Snail and E47 repressors of E-cadherin induce distinct invasive and angiogenic properties in vivo. *J Cell Sci* 2004; **117**: 2827-2839.

9. Cubillo M, Diaz-Lopez A, Cuevas EP, Moreno-Bueno G, Peinado H, Montes A *et al*. E47 and id1 interplay in epithelial-mesenchymal transition. *PLOsOne* 2013; **8(3)**: e59948.

10. De Craene B, Berx G. Regulatory networks defining EMT during cancer initiation and progression. *Nat Rev Cancer* 2013; **13**: 97-110.

11. Peinado H, Iglesias-de la Cruz MC, Olmeda D, Csiszar K, Fong KS, Vega S *et al*. A molecular role for lysyl oxidase-like 2 enzyme in snail regulation and tumor progression. *EMBO J* 2005; **24**: 3446-3458.

12. Peinado H, Moreno-Bueno G, Hardisson D, Pérez-Gómez E, Santos V, Mendiola M *et al*. Lysyl oxidase-like 2 as a new poor prognosis marker of squamous cell carcinomas. *Cancer Res* 2008; **68**: 4541-4550.

13. Moreno-Bueno G, Salvador F, Martín A, Floristán A, Cuevas EP, Santos V *et al*. Lysyl oxidase-like 2 (LOXL2), a new regulator of cell polarity required for metastatic dissemination of basal-like breast carcinomas. *EMBO Mol Med* 2011; **3**: 528-544.

14. Csiszar K. Lysyl oxidases: a novel multifunctional amine oxidase family. *Prog Nucleic Acid Res Mol Biol* 2001; **70**: 1-32.

15. Mäki JM, Räsänen J, Tikkanen H, Sormunen R, Mäkikallio K, Kivirikko KI *et al*. Inactivation of the lysyl oxidase gene Lox leads to aortic aneurysms, cardiovascular dysfunction, and perinatal death in mice. *Circulation* 2002; **106**: 2503-2509.

16. Liu X, Zhao Y, Gao J, Pawlyk B, Starcher B, Spencer JA *et al*. Elastic fiber homeostasis requires lysyl oxidase-like 1 protein. *Nat Genet* 2004; **36**:178-182.

17. Barker HE, Cox TR, Erler JT. The rationale for targeting the LOX family in cancer. *Nat Rev Cancer* 2012; **12**: 540-552.

18. Cano A, Santamaria PG, Moreno-Bueno G. LOXL2 in epithelial cell plasticity and tumor progression. *Future Oncol* 2012; **8**: 1095-1108.

19. Barker HE, Chang J, Cox TR, Lang G, Bird D, Nicolau M *et al*. LOXL2-mediated matrix remodeling in metastasis and mammary gland involution. *Cancer Res* 2011; **71**: 1561-1572.

20. Psaila B, Lyden D. The metastatic niche: adapting the foreign soil. *Nat Rev Cancer* 2009; **9**: 285-293.

21. Kaplan RN, Riba RD, Zacharoulis S, Bramley AH, Vincent L, Costa C *et al*. VEGFR1-positive haematopoietic bone marrow progenitors initiate the pre-metastatic niche. *Nature* 2005; **438**: 820-827.

22. Peinado H, Lavotshkin S, Lyden D. The secreted factors responsible for pre-metastatic niche formation: Old sayings and new thoughts. *Semin Cancer Biol* 2011; **21**: 139-146.

23. Erler JT, Bennewith KL, Nicolau M, Dornhöfer N, Kong C, Le QT *et al*. Lysyl oxidase is essential for hypoxia-induced metastasis. *Nature* 2006; **440**: 1222-1226.

24. Erler JT, Bennewith KL, Cox TR, Lang G, Bird D, Koong A *et al*. Hypoxia-induced lysyl oxidase is a critical mediator of bone marrow cell recruitment to form the premetastatic niche. *Cancer Cell* 2009; **15**: 35-44.

25. Wong CC, Gilkes DM, Zhang H, Chen J, Wei H, Chaturvedi P *et al*. Hypoxia-inducible factor 1 is a master regulator of breast cancer metastatic niche formation. *Proc Natl Acad Sci USA* 2011; **108**: 16369-16374.

26. Cuevas EP, Moreno-Bueno G, Canesin G, Santos V, Portillo F, Cano A. LOXL2 catalytically inactive mutants mediate epithelial-to-mesenchymal transition. *Biology Open* 2013 (*in press*).

27. Massari ME, Jennings PA, Murre C. The AD1 transactivation domain of E2A contains a highly conserved helix which is required for its activity in both Saccharomyces cerevisiae and mammalian cells. *Mol Cell Biol* 1996; **16**: 121-129.

28. Ewens A, Mihich E, Ehrke MJ. Distant metastasis from subcutaneously grown E0771 medullary breast adenocarcinoma. *Anticancer Res* 2005; **25**: 3905-3915.

29. Hiratsuka S, Watanabe A, Aburatani H, Maru Y. Tumour-mediated upregulation of chemoattractants and recruitment of myeloid cells predetermines lung metastasis. *Nat Cell Biol* 2006; **8**: 1369-1375.

30. Bosiljcic M, Hamilton MJ, Banath JP, LePard, NE, McDougal DC, Jia JX *et al*. Myeloid suppressor cells regulate the lung environment-Letter. *Cancer Res* 2011; **71**: 5050-5051

31. Hiratsuka S, Watanabe A, Sakurai Y, Akashi-Takamura S, Ishibashi S, Miyake K *et al*. The S100A8-serum amyloid A3-TLR4 paracrine cascade establishes a pre-metastatic phase. *Nat Cell Biol* 2008; **10**: 1349-1355.

32. Oskarsson T, Acharyya S, Zhang XH, Vanharanta S, Tavazoie SF, Morris PG *et al*. Breast cancer cells produce tenascin C as a metastatic niche component to colonize the lungs. *Nat Med* 2011; **17**: 867-874.

33. Peng L, Ran YL, Hu H, Yu L, Liu Q, Zhou Z *et al*. Secreted LOXL2 is a novel therapeutic target that promotes gastric cancer metastasis via the Src/FAK pathway. *Carcinogenesis* 2009; **30**: 1660-1669.

34. Barry-Hamilton V, Spangler R, Marshall D, McCauley S, Rodriguez HM, Oyasu M *et al*. Allosteric inhibition of lysyl oxidase-like-2 impedes the development of a pathologic microenvironment. *Nat Med* 2010; **16**: 1009-1017.

35. Ocaña OH, Córcoles R, Fabra A, Moreno-Bueno G, Acloque H, Vega S *et al*. Metastatic colonization requires the repression of the epithelial-mesenchymal transition inducer Prrx1. *Cancer Cell* 2012; **22**:709-724.

36. Tsai JH, Donaher JL, Murphy DA, Chau S, Yang J. Spatiotemporal regulation of epithelial-mesenchymal transition is essential for squamous cell carcinoma metastasis. *Cancer Cell* 2012; **22**:725-736.

37. Gao D, Joshi N, Choi H, Ryu S, Hahn M, Catena R *et al*. Myeloid progenitor cells in the premetastatic lung promote metastasis by inducing mesenchymal to epithelial transition. *Cancer Res* 2012; **72**: 1384-1394.

38. Ye XZ, Yu SC, Bian XW. Contribution of myeloid-derived suppressor cells to tumor-induced immune suppression, angiogenesis, invasion and metastasis. *J Genet Genomics* 2010; **37**: 423-430.

39. Sceneay J, Chow MT, Chen A, Halse HM, Wong CS, Andrews DM *et al*. Primary Tumor Hypoxia Recruits CD11b+/Ly6Cmed/Ly6G+ Immune Suppressor Cells and Compromises NK Cell Cytotoxicity in the Premetastatic Niche. *Cancer Res* 2012; **72**: 3906-3911.

40. Fogelgren B, Polgár N, Szauter KM, Ujfaludi Z, Laczkó R, Fong KS *et al*. Cellular fibronectin binds to lysyl oxidase with high affinity and is critical for its proteolytic activation. *J Biol Chem* 2005; **280**: 24690-24697.

41. Cox TR, Bird D, Baker AM, Barker HE, Ho MW, Lang G *et al*. LOX-mediated collagen crosslinking is responsible for fibrosis-enhanced metastasis. *Cancer Res* 2013; **73**: 1721-1732.

42. Peinado H, Alečković M, Lavotshkin S, Costa-Silva B, Moreno-Bueno G, Hergueta-Redondo M

et al. Melanoma-derived exosomes educate bone marrow progenitor cells toward a pro-metastatic phenotype through upregulation of the MET oncoprotein. *Nat Med* 2012; **18**: 883-891.

43. Moreno-Bueno G, Peinado H, Molina P, Olmeda D, Cubillo E, Santos V *et al*. The morphological and molecular features of the epithelial-to-mesenchymal transition. *Nat Protoc* 2009; **4**: 1591-1613.

Figure Legends

Figure 1: LOXL2 functionally interacts with E47. (**a**) and (**d**) Coimmunoprecipitation assays in (**a**) MDCK-EGFP-E47 cells transiently transfected with LOXL2-Flag, or (**d**) MDA-MB231 and Eo771 cells. Cell extracts were immunoprecipitated with anti-EGFP, anti-Flag or anti-LOXL2 and analyzed by WB with anti-LOXL2 or anti-EGFP (**a**), anti-LOXL2 or anti-E2A antibodies (**d**). Left panels show input levels of indicated proteins. LOXL2-Flag, EGFP-E47, endogenous LOXL2 and E2A, and control IgG are indicated. Data show one representative experiment out of two. (**b**) Pull-down assay**.** HEK293T cells were transiently transfected with LOXL2-Flag and cell extracts incubated with GST-E47 or GST. LOXL2-Flag and GST-E47 proteins were detected by WB with anti-Flag and anti-GST antibodies, respectively. Left insert shows input LOXL2-Flag level. (**c**) Co-localization of endogenous E47 (E2A) with LOXL2-Flag in MDCK-LOXL2-Flag cells (upper, merged images) and E-cadherin stain in parental MDCK and MDCK-LOXL2-Flag cells (bottom) analyzed by confocal immunofluorescence with anti-Flag, anti-E-cadherin (green) or anti-E2A antibodies (red). Nuclei stained with DAPI. Amplified image (upper right) shows LOXL2/E47 co-localization in the perinuclear region. Bar, 20 µm. (**e**) and (**f)** Activity of *E-Cadherin* promoter in HEK293T cells in the presence of wt-E47 or E47ΔAD1 (100 ng) and/or wt LOXL2-Flag or LOXL2ΔCD-Flag (50 ng). Activity (RLU) was normalized to control pcDNA3 vector. Results represent the mean +/- SD of at least

three independent experiments performed in triplicate samples. **0.001<p<0.005, ***p<0.001, ns=not significant.

Figure 2: LOXL2 or E47 silencing in Eo771 cells reduces tumor growth and dramatically decreases lung metastasis. (**a**) Representative bioluminescence images of C57Bl/6j mice injected in the mfp with Eo771pLKO, shLOXL2 (clone #3) or shE47 (414*pool*) cells, at 7 and 15 dpi. (**b**) Primary tumor growth of Eo771pLKO, shLOXL2 or shE47 cells at the indicated dpi, assessed by tumor volume. n=6 mice/group. (**c**) Histology of representative primary tumors (left) and lungs (right) from pLKO, shLOXL2#3 or shE47-416#4 Eo771 injected mice (x20) at 24 dpi, insets show amplified areas (x40). (**d**) Representative bioluminescence images of lungs and (**e**) quantification of total lung photon flux of Eo771pLKO, shLOXL2 or shE47 mfp injected mice at 24 dpi. n=6 mice/group. (**f**) Representative bioluminescence images of lungs and (**g**) quantification of total lung photon flux 5 weeks after tail vein injection of Eo771pLKO, shLOXL2 or shE47 cells in C57BL/6J mice. n=6 mice/group. (**h**) Representative bioluminescence images (15 dpi) and (**i**) primary tumor growth by volume of C57Bl/6 mice injected in the mfp with Eo771pLKO, shE47-416#4, and shE47-416#4 cells transfected with control pcDNA3 or LOXL2-HA. n= 4 mice/group. (**j**) Representative histological sections of lungs of C57Bl/6 mice injected in the mfp with the indicated Eo771 cells at 15 dpi. Asterisks indicated metastasis foci. Color scales represent the photon flux (photons per second) emitted from the tumor region (**a** and **h**) or dissected lungs (**d** and **f**). Data in (**b, e, g,** and **i**) show the mean +/- SD. *p<0.05, **0.001<p<0.005, ***p<0.001, n.s., non-significant.

Figure 3 Tumorigenic and lung metastatic behavior of 4T1 cells after E47 silencing or LOXL2 overexpression. (**a**) and (**g**) Western blot analyses of E47, LOXL2 and the indicated markers in wt 4T1 cells, and after E47 silencing (sh414 and sh416 pools) (**a**) or LOXL2 overexpression (**g**) and corresponding controls (pLKO and pcDNA3, respectively). (**b**) and (**c**) Bioluminescence images (21

dpi) (**b**) and primary tumor growth assessed by volume (**c**) of Balb/C mice injected in the mfp with control 4T1pLKO and shE47 (414 and 416 pools) cells. n=5 mice/group. (**d**) and (**e**) Bioluminescence images (**d**) and quantification of total lung photon flux (**e**) of lungs from Balb/C mice mfp injected with control 4T1pLKO and shE47 (414 and 416 pools) cells at 21 dpi. n=5 mice/group. (**f**) Representative histological sections of primary tumors (left) and lungs (right) of Balb/C mice mfp injected with the indicated 4T1 controls and shE47 or LOXL2 overexpressing pools. Asterisks indicated metastasis foci. (**h-j**) Primary tumor growth assessed by volume (**h**), representative bioluminescence images of lungs (**i**) and quantification of total lung photon flux (**j**) from Balb/C mice injected in the mfp with control 4T1pcDNA3 and LOXL2-HA cells at 28 dpi. n=4 mice/group. Color scales represent the photon flux (photons per second) emitted from the tumor region (**b**) or dissected lungs (**d** and **i**). Data in (**c, e**, **h** and **j**) show the mean +/-SD. *p<0.05, **0.001<p<0.005, n.s., non-significant.

Figure 4: LOXL2 and E47 required for BMDCs recruitment to lung. (**a**) Confocal analysis of BMDC-eGFP$^+$ (green) and Eo771 tumor mCherry$^+$ cells (red) in the lungs. C57BL/6J mice were transplanted with eGFP$^+$ BM cells, injected into the mfp with wt Eo771, pLKO, shLOXL2 (clones #3 and #8) or shE47 (414*pool* and clone 416#4) cells and lungs analyzed 15 dpi. Nuclei were stained with DAPI. Representative images are shown for each experimental group. Bar, 100 µm. Amplified images are shown in the right panels. (**b**) and (**c**) Quantification of the total number of BMDC-GFP$^+$ (green) (**b**) and metastatic mCherry$^+$ cells (red) (**c**) per field area in each independent group, including non-injected mice (NI), n=3 mice/group. Data show the mean +/-SD. **0.001<p<0.005, ***p<0.001 by ANOVA.

Figure 5: LOXL2 and E47 are required for mobilization and lung recruitment of BMPC. FACS analysis and relative quantification of myeloid (CD11b$^+$/Gr-1$^+$) and BMPC (c-kit$^+$/Sca-1$^+$) cells in

blood and lungs of mice injected with Eo771 and 4T1 cells. (**a-f**) C57Bl/6 mice were injected into the mfp with wtEo771, pLKO, shLOXL2 and shE47 cells (**a, b, d, e**) or pLKO, shE47-416#4 (shE47) and shE47-416#4 cells transfected with control pcDNA3 or LOXL2-HA (**c, f**). Blood (**a, d**) and lungs (**b, c, e, f**) were analyzed at 15 dpi, compared to not injected (NI) mice. n=3-6 mice/group. (**g-n**) Balb/C mice were injected into the mfp with 4T1pLKO cells and after silencing for E47 (sh414 and sh416 pools) (**g, h, k, l**) or 4T1 cells transfected with control pcDNA3 or LOXL2-HA (**i, j, m, n**); blood (**g, i, k, m**) and lungs (**h, j, l, n**) were analyzed at 21 dpi. n=3-5 mice/group. Results represent the mean +/-SD of one or two independent experiments. *p<0.05, **0.001<p<0.005, ***p<0.001, ns=not significant.

Figure 6: LOXL2 and E47 regulate the expression of fibronectin and LOX members. qPCR analysis of *E47*, *Fibronectin* (FN) and *LOX* members in primary tumors (**a**) and lungs (**b-d**) of C57Bl/6j (**a-c**) and Balb/C (**d**) mice injected into the mfp with (**a, b**) Eo771pLKO, shLOXL2 (clones #3 and #8) or shE47 (414*pool* and clone 416#4) cells, and (**c**) Eo771pLKO, shE47-416#4, and shE47-416#4 cells transfected with control pcDNA3 or LOXL2-HA at 15 dpi; **(d)** lungs from Balcb/C mice injected with 4T1 cells transfected with control pcDNA3 or LOXL2-HA at 21 dpi. n=3-6 mice/group. Results represent the mean +/-SD *p<0.05, **0.001<p<0.005, ***p<0.001, ns=not significant.

Figure 7: LOXL2 and E47 regulate the expression of cytokines involved in pre-metastatic niche formation. (**a**) Cytokine array incubated with conditioned media from Eo771pLKO, shLOXL2 (clone #3) and shE47 (414*pool*) cells. Factors decreased in both shLOXL2 and shE47 cells are indicated by black boxes (A6: ANG-1; C4: GM-CSF). (**b-e**) qPCR of *GM-CSF*, *TGFβ*, *TNFα*, *TEN-C*, *ANG-1, S100A8* and *S100A9* in Eo771shpLKO, shLOXL2 or shE47 cells in culture (**b**), primary tumors (**c**) and/or lungs (**d, e**) of C57Bl/6 mice injected into the mfp with the indicated Eo771 cells at 15 dpi. (**f**) qPCR of the indicated cytokines in lungs from BalB/C mice injected with 4T1 cells transfected with

control pcDNA3 and LOXL2-HA at 21 dpi. n=3-6 mice/group. Data show the mean +/-SD. *p<0.05, **0.001<p<0.005, ***p<0.001, ns=not significant. (**g-j**) Activity of the mouse *TNFα* (**g**) and *GM-CSF* (**i**) promoters in the indicated Eo771 cell lines in the absence or presence of 100 nM PMA. Activity of the mouse *TNFα* (**h**) and *GM-CSF* (**j**) promoters in Eo771-shpLKO cells in the presence the indicated amounts (ng) of pcDNA3-E47 and/or pcDNA3-LOXL2. RLU activity was normalized to pLKO cells (**g, i**) or in the presence of pcDNA3 vector (**h, j**). Data represent the mean +/- SD of six (**g, i**) and two (**h, j**) independent experiments performed in triplicate samples. *p<0.05, **0.001<p<0.005, ***p<0.001, ns=not significant.

Figure 8: LOXL2 and E47 cell autonomous action on metastasis and dependence of fibronectin and GM-CSF expression. (**a)** and (**b**) Pre-conditioning of the metastatic niche by mfp injection of C57Bl/6J mice with unlabeled parental Eo771 cells; 10 days later mice were injected with Eo771pLKO- shE47- and shLOXL2-mCherryLuc cells and sacrificed 15 days later. Lung bioluminescence (**a**) and quantication by photon flux (**b**). n=5 mice/group. (**c-f**) Eo771shControl cells or interfered for fibronectin (shFN) (**c**) were mfp injected in C57Bl/6 mice and lung metastasis assessed by biolumiscence (**d**) and quantification of photon flux (**e**) at 24 dpi; (f) qPCR of *GM-CSF* and *TNFα* in lungs from mice injected with Eo771-PLKO and shFN cells. n=6 mice/group. (**g-l**) GM-CSF was silenced in Eo771 cells (**g**) and mfp injected in parallel to pLKO control cells, in C57Bl/6 mice. Bioluminescence images (**h**), tumor growth (**i**) and representative histological lung sections (**j**) at 15 dpi; asterisks in (**j**) indicate metastasis foci; (**k**) and (**l**) qPCR of *fibronectin* and *TNFα* (**k**) and FACS analyses of BMPC and myeloid populations (**l**) in lungs from Eo771pLKO and shGM-GSF-injected mice at 15 dpi. n=5 mice/group. Color scales represent the photon flux (photons per second) emitted from the tumor region (**h**) or dissected lungs (**a, d**). Data in (**b, c, e, f, g, i, k, l**) represent the mean+/-SD. *p<0.05, **0.001<p<0.005, ***p<0.001, ns=not significant.

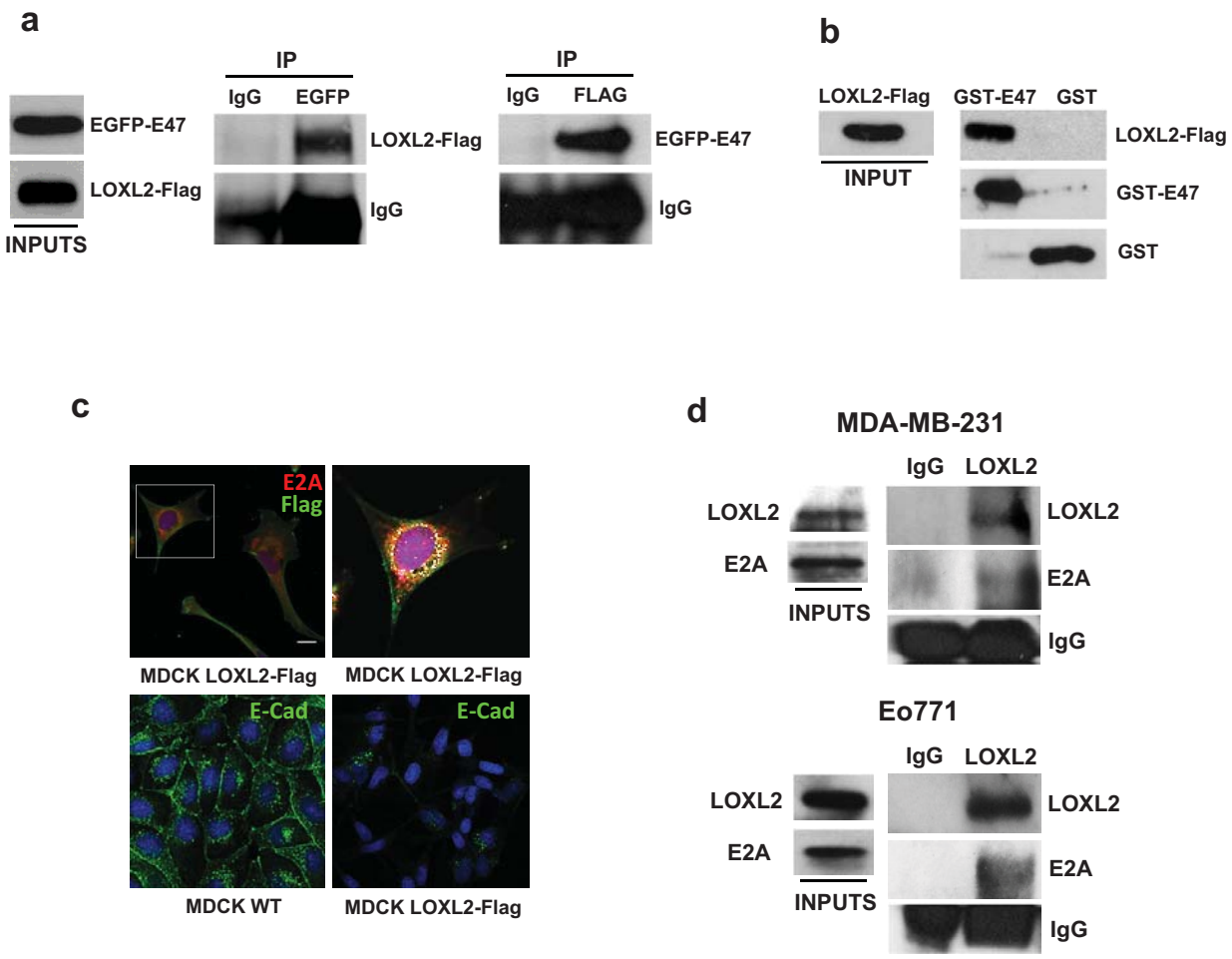
a
IP
IgG
EGFP
EGFP-E47
LOXL2-Flag
INPUTS
LOXL2-Flag
IgG
IP
IgG
FLAG
EGFP-E47
IgG
b
LOXL2-Flag
GST-E47
GST
INPUT
LOXL2-Flag
GST-E47
GST
c
E2A
Flag
MDCK LOXL2-Flag
MDCK LOXL2-Flag
E-Cad
E-Cad
MDCK WT
MDCK LOXL2-Flag
d
MDA-MB-231
IgG
LOXL2
LOXL2
E2A
INPUTS
LOXL2
E2A
IgG
Eo771
IgG
LOXL2
LOXL2
E2A
INPUTS
LOXL2
E2A
IgG
e
**
**
1.00
0.75
0.50
0.25
0.00
E-cadherin promoter activity (RLU)
n.s.
PCDNA3 + + + + - -
E47 - + - - + -
E47ΔAD1 - - + - - +
LOXL2 - - - + + +
f
**
***
1.00
0.75
0.50
0.25
0.00
E-cadherin promoter activity (RLU)
n.s.
PCDNA3 + + + + - -
E47 - + - - + +
LOXL2 WT - - + - + -
LOXL2 ΔCD - - - + - +

Figure 1

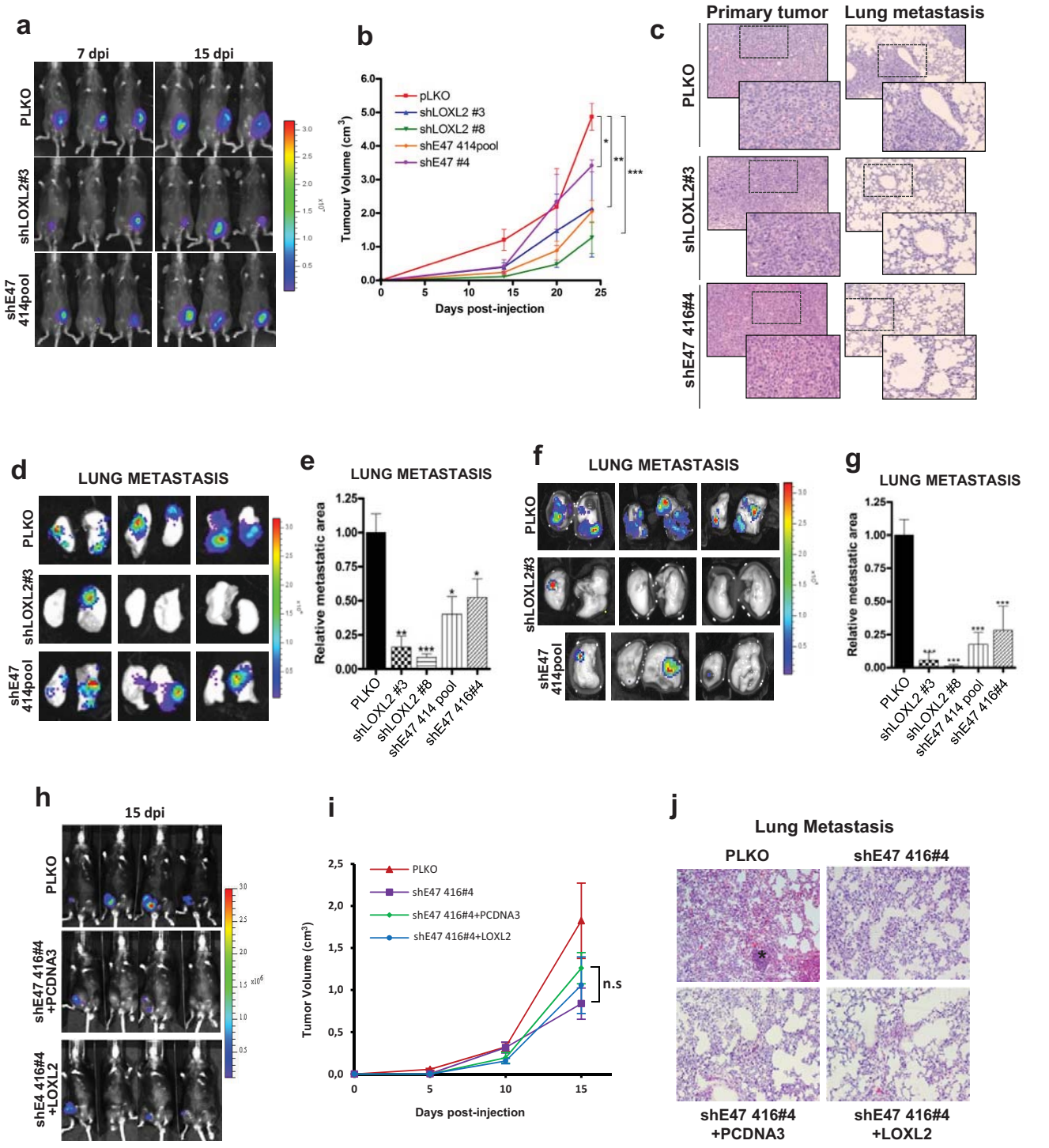
a
7 dpi
15 dpi
PLKO
shLOXL2#3
shE47 414pool
b
pLKO
shLOXL2 #3
shLOXL2 #8
shE47 414pool
shE47 #4
Tumour Volume (cm3)
Days post-injection
c
Primary tumor
Lung metastasis
PLKO
shLOXL2#3
shE47 416#4
d
LUNG METASTASIS
PLKO
shLOXL2#3
shE47 414pool
e
LUNG METASTASIS
Relative metastatic area
PLKO
shLOXL2 #3
shLOXL2 #8
shE47 414 pool
shE47 416#4
f
LUNG METASTASIS
PLKO
shLOXL2#3
shE47 414pool
g
LUNG METASTASIS
Relative metastatic area
PLKO
shLOXL2 #3
shLOXL2 #8
shE47 414 pool
shE47 416#4
h
15 dpi
PLKO
shE47 416#4 +PCDNA3
shE4 416#4 +LOXL2
i
PLKO
shE47 416#4
shE47 416#4+PCDNA3
shE47 416#4+LOXL2
Tumor Volume (cm3)
n.s
Days post-injection
j
Lung Metastasis
PLKO
shE47 416#4
shE47 416#4 +PCDNA3
shE47 416#4 +LOXL2

Figure 2

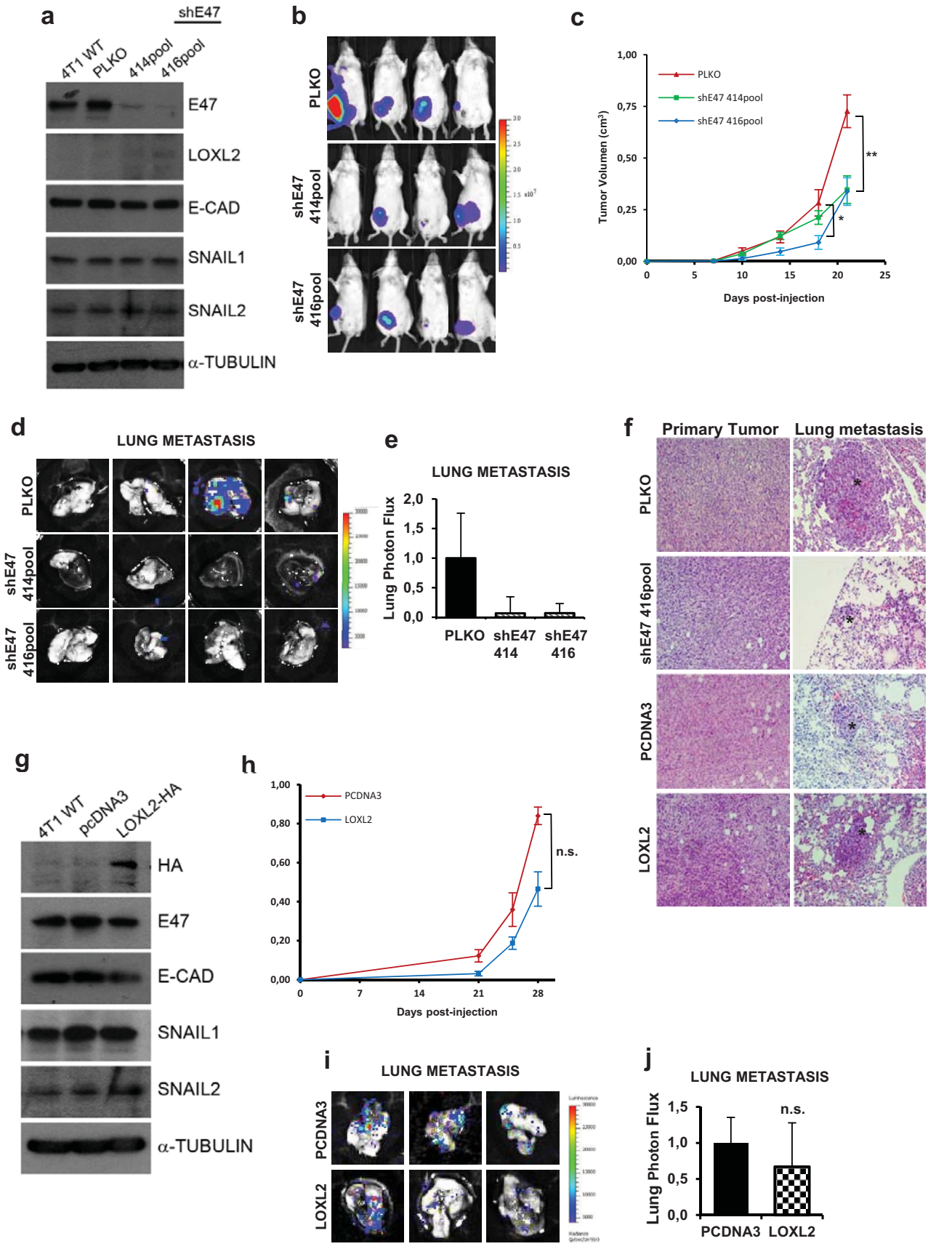
a
shE47
4T1 WT
PLKO
414pool
416pool
E47
LOXL2
E-CAD
SNAIL1
SNAIL2
α-TUBULIN
b
PLKO
shE47 414pool
shE47 416pool
c
PLKO
shE47 414pool
shE47 416pool
Tumor Volumen (cm³)
Days post-injection
d
LUNG METASTASIS
PLKO
shE47 414pool
shE47 416pool
e
LUNG METASTASIS
Lung Photon Flux
PLKO
shE47 414
shE47 416
f
Primary Tumor
Lung metastasis
PLKO
shE47 416pool
PCDNA3
LOXL2
g
4T1 WT
pcDNA3
LOXL2-HA
HA
E47
E-CAD
SNAIL1
SNAIL2
α-TUBULIN
h
PCDNA3
LOXL2
n.s.
Days post-injection
i
LUNG METASTASIS
PCDNA3
LOXL2
j
LUNG METASTASIS
Lung Photon Flux
n.s.
PCDNA3
LOXL2

Figure 3

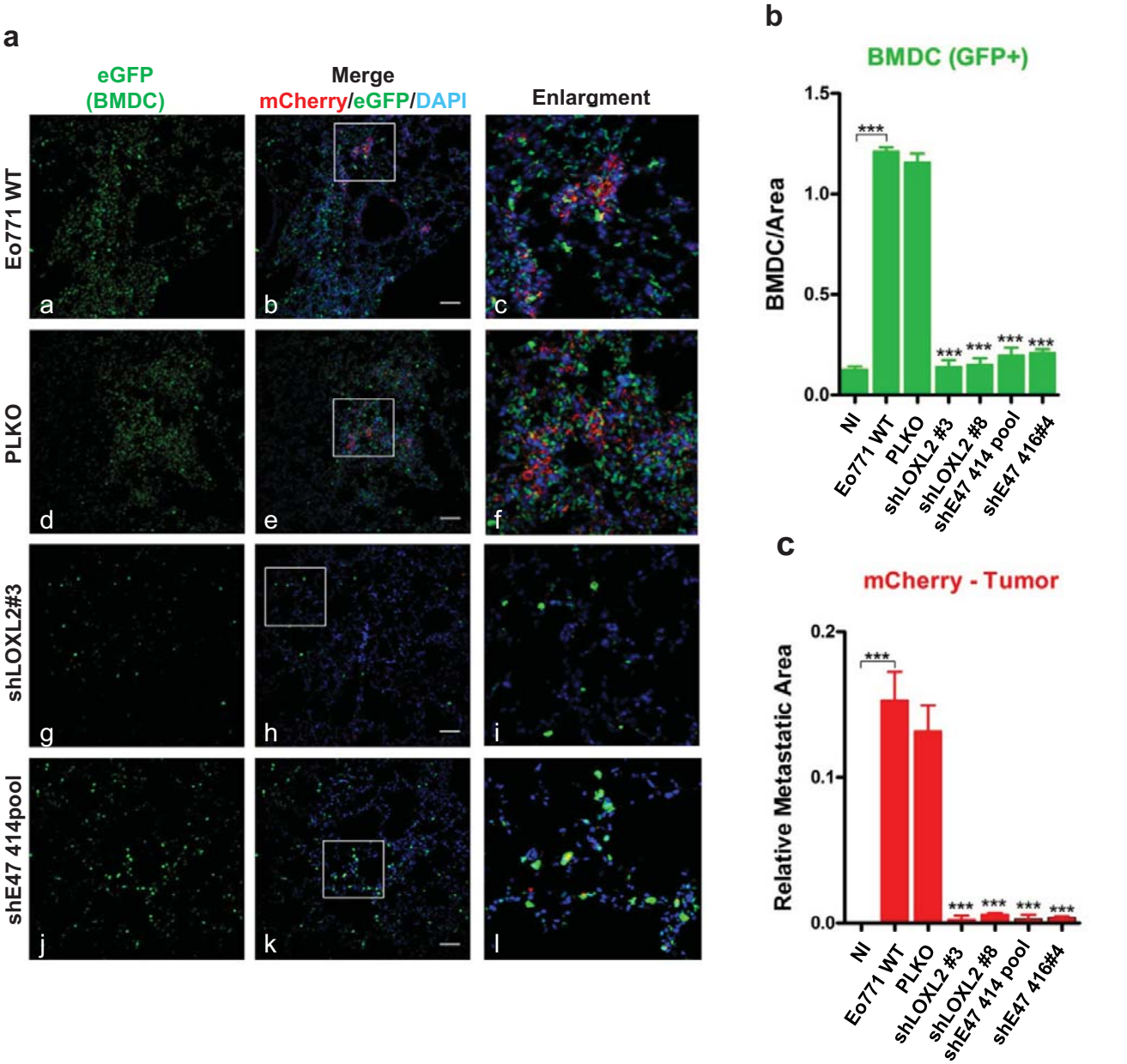
a
eGFP (BMDC)
Merge mCherry/eGFP/DAPI
Enlargment
Eo771 WT
PLKO
shLOXL2#3
shE47 414pool
a
b
c
d
e
f
g
h
i
j
k
l
b
BMDC (GFP+)
BMDC/Area
1.5
1.0
0.5
0.0
***
NI
Eo771 WT
PLKO
shLOXL2 #3
shLOXL2 #8
shE47 414 pool
shE47 416#4
c
mCherry - Tumor
Relative Metastatic Area
0.2
0.1
0.0

Figure 4

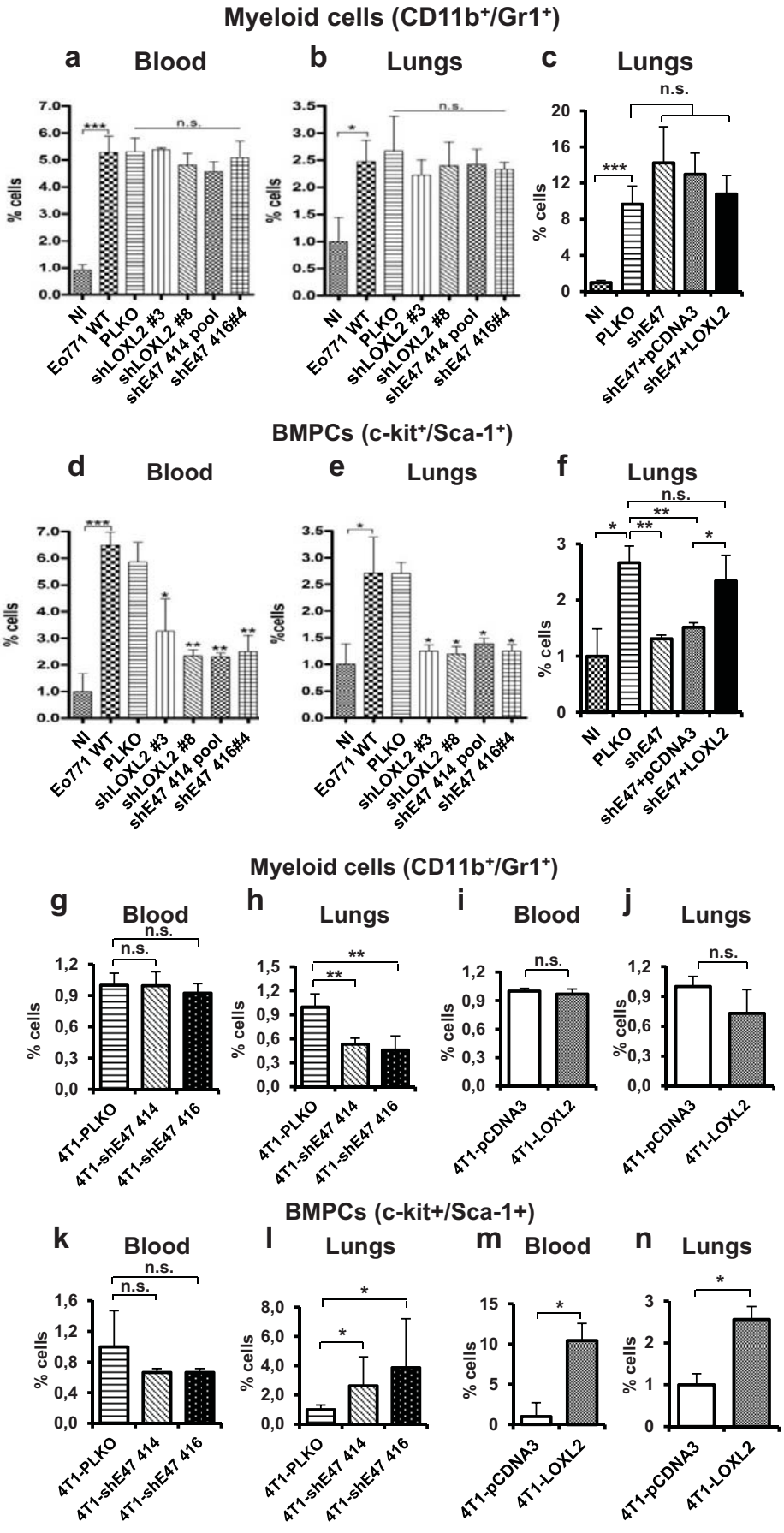
Myeloid cells (CD11b+/Gr1+)
a Blood
b Lungs
c Lungs
% cells
NI
Eo771 WT
PLKO
shLOXL2 #3
shLOXL2 #8
shE47 414 pool
shE47 416#4
shE47
shE47+pCDNA3
shE47+LOXL2
n.s.
BMPCs (c-kit+/Sca-1+)
d Blood
e Lungs
f Lungs
Myeloid cells (CD11b+/Gr1+)
g Blood
h Lungs
i Blood
j Lungs
4T1-PLKO
4T1-shE47 414
4T1-shE47 416
4T1-pCDNA3
4T1-LOXL2
BMPCs (c-kit+/Sca-1+)
k Blood
l Lungs
m Blood
n Lungs

Figure 5

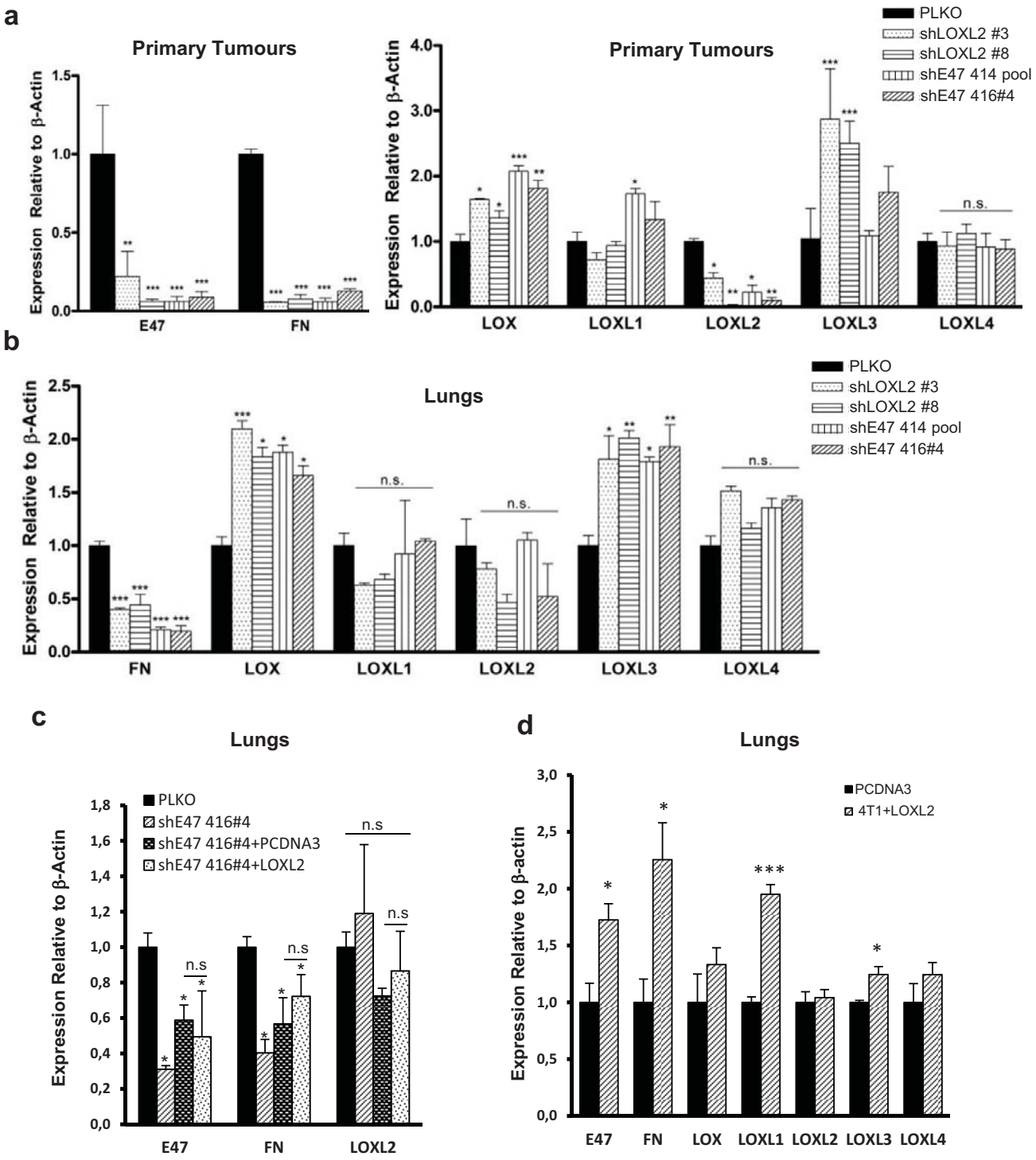
a
Primary Tumours
Expression Relative to β-Actin
E47
FN
Primary Tumours
LOX
LOXL1
LOXL2
LOXL3
LOXL4
n.s.
PLKO
shLOXL2 #3
shLOXL2 #8
shE47 414 pool
shE47 416#4
b
Lungs
FN
LOX
LOXL1
LOXL2
LOXL3
LOXL4
c
Lungs
shE47 416#4+PCDNA3
shE47 416#4+LOXL2
d
Lungs
PCDNA3
4T1+LOXL2

Figure 6

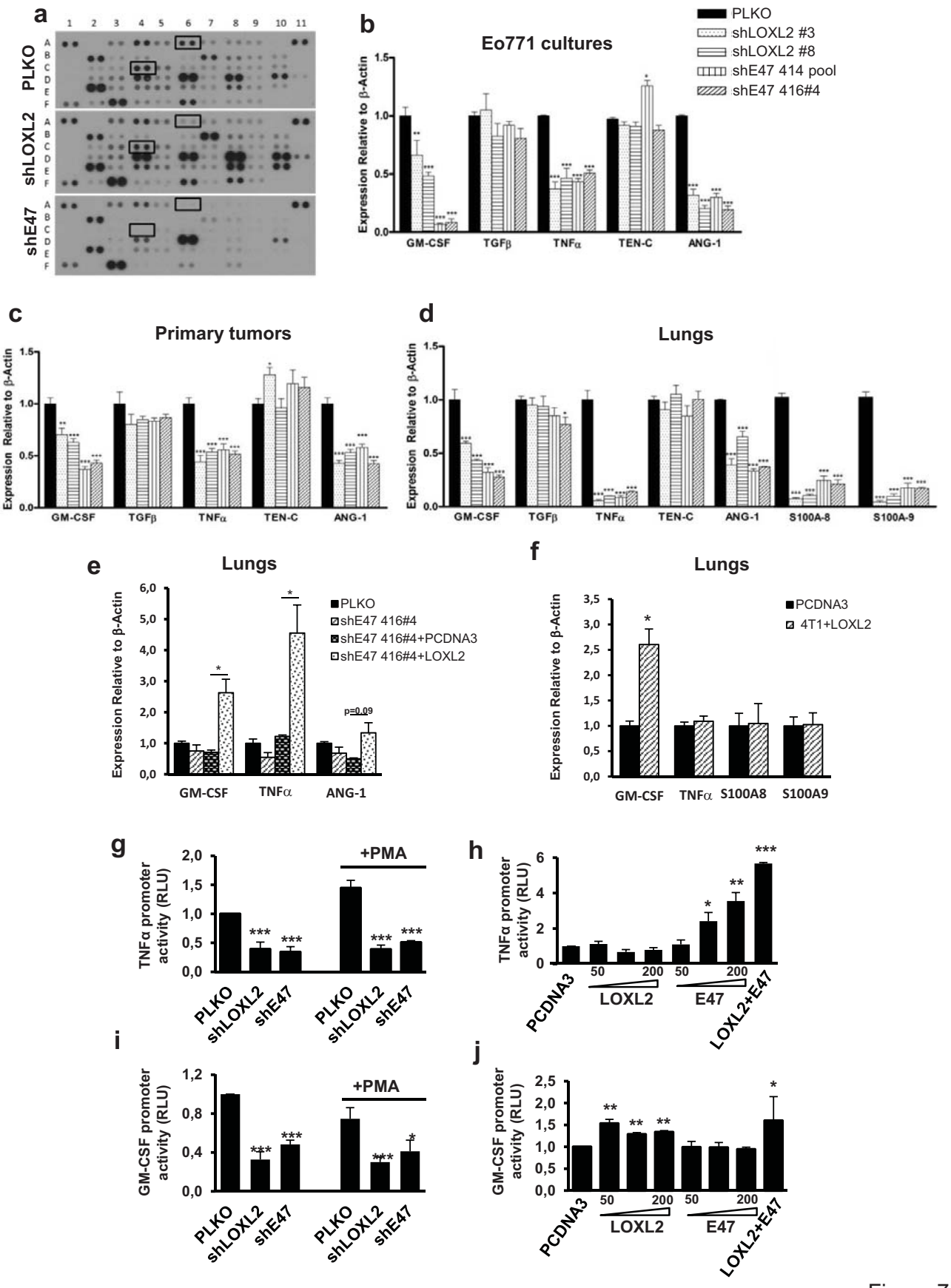
a
PLKO
shLOXL2
shE47
b
Eo771 cultures
PLKO
shLOXL2 #3
shLOXL2 #8
shE47 414 pool
shE47 416#4
Expression Relative to β-Actin
GM-CSF
TGFβ
TNFα
TEN-C
ANG-1
c
Primary tumors
d
Lungs
S100A-8
S100A-9
e
Lungs
PLKO
shE47 416#4
shE47 416#4+PCDNA3
shE47 416#4+LOXL2
p=0.09
f
Lungs
PCDNA3
4T1+LOXL2
S100A8
S100A9
g
TNFα promoter activity (RLU)
+PMA
PLKO
shLOXL2
shE47
h
PCDNA3
LOXL2
E47
LOXL2+E47
i
GM-CSF promoter activity (RLU)
j

Figure 7

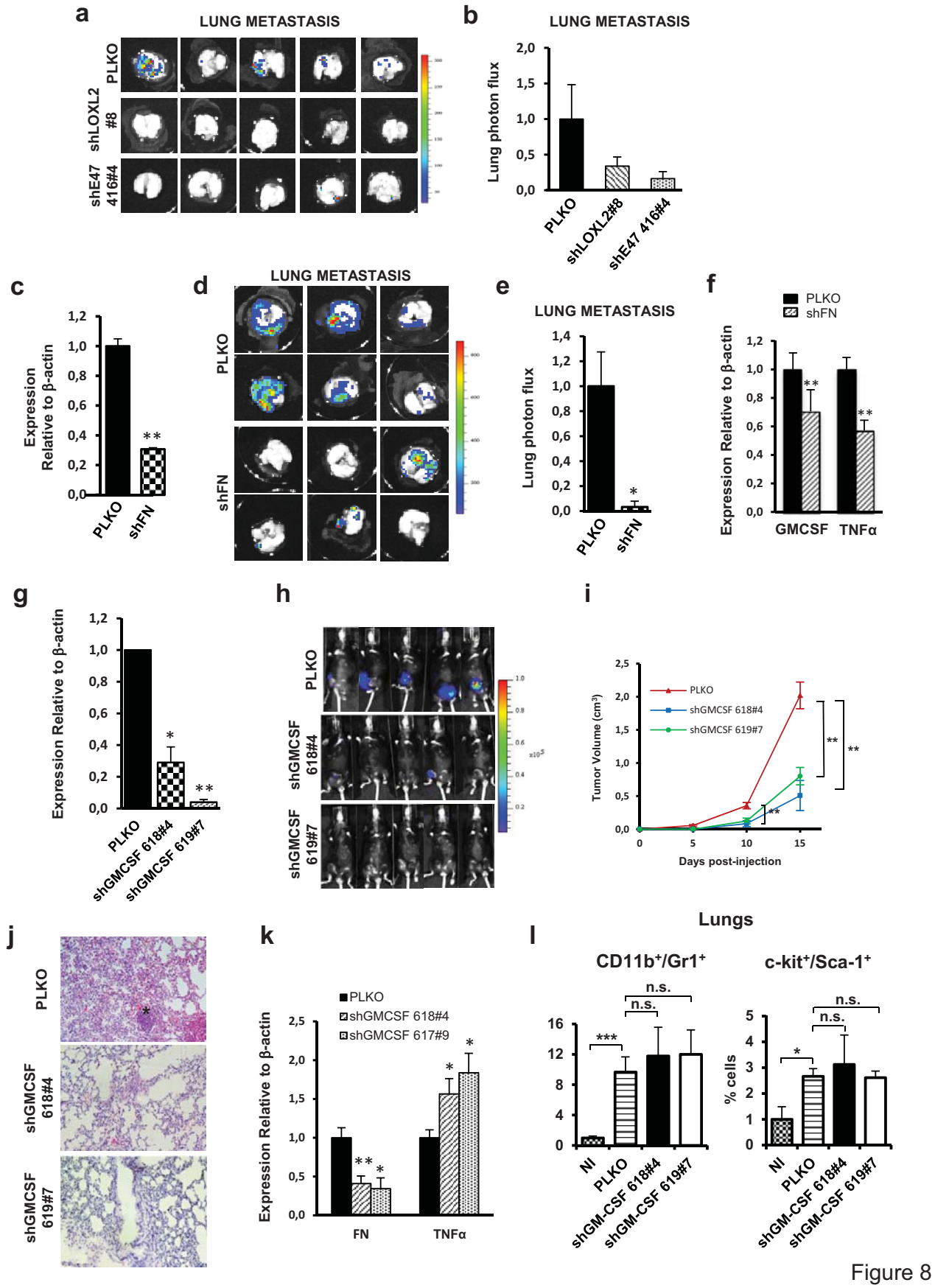
a
LUNG METASTASIS
PLKO
shLOXL2 #8
shE47 416#4
b
LUNG METASTASIS
Lung photon flux
2,0
1,5
1,0
0,5
0,0
PLKO
shLOXL2#8
shE47 416#4
c
Expression Relative to β-actin
1,2
1,0
0,8
0,6
0,4
0,2
0,0
**
PLKO
shFN
d
LUNG METASTASIS
PLKO
shFN
e
LUNG METASTASIS
Lung photon flux
1,4
1,2
1,0
0,8
0,6
0,4
0,2
0,0
*
PLKO
shFN
f
PLKO
shFN
Expression Relative to β-actin
1,2
1,0
0,8
0,6
0,4
0,2
0,0
**
**
GMCSF
TNFα
g
Expression Relative to β-actin
1,2
1,0
0,8
0,6
0,4
0,2
0,0
*
**
PLKO
shGMCSF 618#4
shGMCSF 619#7
h
PLKO
shGMCSF 618#4
shGMCSF 619#7
i
Tumor Volume (cm³)
2,5
2,0
1,5
1,0
0,5
0,0
PLKO
shGMCSF 618#4
shGMCSF 619#7
**
**
**
0
5
10
15
Days post-injection
j
PLKO
shGMCSF 618#4
shGMCSF 619#7
*
k
PLKO
shGMCSF 618#4
shGMCSF 617#9
Expression Relative to β-actin
2,5
2,0
1,5
1,0
0,5
0,0
**
*
*
*
FN
TNFα
l
Lungs
CD11b⁺/Gr1⁺
c-kit⁺/Sca-1⁺
n.s.
n.s.
***
n.s.
n.s.
*
% cells
16
12
8
4
0
5
4
3
2
1
0
NI
PLKO
shGM-CSF 618#4
shGM-CSF 619#7

Figure 8